

Cite this: *Chem. Sci.*, 2025, 16, 13468

All publication charges for this article have been paid for by the Royal Society of Chemistry

Received 15th April 2025
Accepted 16th June 2025

DOI: 10.1039/d5sc02780b

rsc.li/chemical-science

Introduction

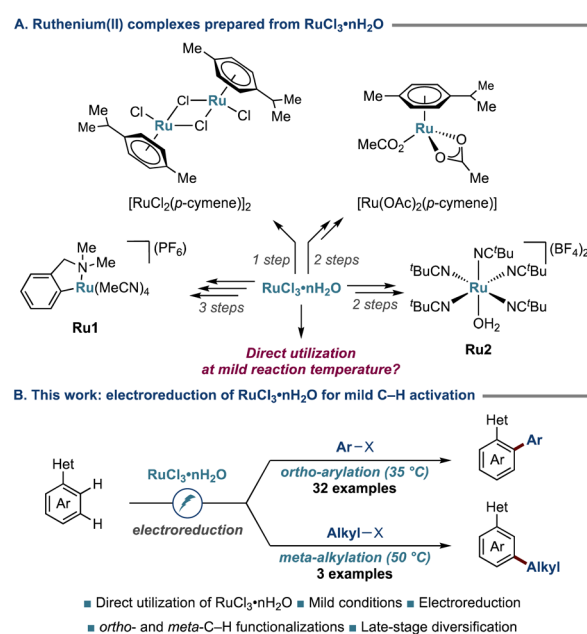
Ruthenium-catalyzed C–H activation chemistry has evolved into an indispensable chemical toolbox for selectively functionalizing arene scaffolds.^{1–10} For instance, site-selectivity can be precisely modulated^{11–17} without exploiting elaborate auxiliaries, providing instant access to *ortho*-^{18–27} or *meta*-decorated frameworks.^{28–41} Our group indeed discovered that the addition of phosphine ligands can alter the site-selectivity in C–H benzylations from *ortho*- to unusual *meta*-selectivities.¹⁴ Precise selectivity control can also be achieved depending on the nature of the electrophilic substrates.^{13,16} Among such transformations, C–H arylations hold a significant potential for the assembly of valuable biaryl scaffolds,^{6,9,10} with carboxylate-assisted ruthenium(II/IV)-catalyzed C–H activations representing the most robust and efficient strategy.²³ In recent years, substantial efforts have been made to render reaction conditions milder. Notable advancements include the use of light irradiation, as disclosed by Ackermann and Greaney,^{42–45} as well as the employment of arene ligand-free ruthenium precatalysts.^{46,47}

Despite the considerable progress,^{48–52} the majority of existing approaches heavily depend on ruthenium(II) precatalysts, which require lengthy organometallic syntheses by experts with

Electroreductive room-temperature C–H activations with $\text{RuCl}_3 \cdot n\text{H}_2\text{O}$ precatalyst *via* cathodic ruthenium(III/II) manifold†Takuya Michiyuki,^a Tristan von Münchow,^a Zhipeng Lin,^a Binbin Yuan,^a João C. A. Oliveira^a and Lutz Ackermann^{a,b}

We, herein, disclose a strategy to directly utilize user-friendly $\text{RuCl}_3 \cdot n\text{H}_2\text{O}$ for *ortho*- as well as *meta*-C–H functionalizations at low temperatures. The key to success was the *in situ* formation of the active ruthenium catalyst through cathodic electron transfer, setting the stage for C–H activations under exceedingly mild reaction conditions. The robustness of our electrocatalysis process was highlighted by the late-stage diversification of compounds of relevance to chemical, agrochemical, and pharmaceutical industries, as well as simple amines as terminal reductants for the electroreduction. Detailed mechanistic studies by, among others, spectroelectrochemical analysis provided strong evidence for a cathodic reduction manifold.

glovebox techniques. This reliance jeopardizes the resource efficiency and user-friendly nature of the overall processes. Importantly, when tracing back the synthesis routes, one can realize that ruthenium(II) complexes, such as $[\text{RuCl}_2(p\text{-cymene})]_2$, $[\text{Ru}(\text{OAc})_2(p\text{-cymene})]$, arene ligand-free complexes **Ru1** and **Ru2**, originate from $\text{RuCl}_3 \cdot n\text{H}_2\text{O}$ (Scheme 1A).^{46,47,53}



Scheme 1 (A) Ruthenium(II) complexes prepared from $\text{RuCl}_3 \cdot n\text{H}_2\text{O}$. (B) This study. Het: heterocycle.

^aWöhler Research Institute for Sustainable Chemistry, Georg-August-Universität Göttingen, Tammannstraße 2, 37077, Göttingen, Germany. E-mail: Lutz.Ackermann@chemie.uni-goettingen.de

^bDZHK (German Centre for Cardiovascular Research), Potsdamer Straße 58, 10875 Berlin, Germany

† Electronic supplementary information (ESI) available. See DOI: [10.1039/d5sc02780b](https://doi.org/10.1039/d5sc02780b)



Table 1 Reaction optimization^a

Entry	Deviations from the above conditions	3 (%) ^b
1	None	90 (85) ^c
2	Room temperature	37
3	NMP instead of DMA	78
4	Aryl iodide or aryl chloride instead of 2a	60/73
5	No electricity but with electrodes	N.D.
6	No RuCl ₃ ·nH ₂ O	N.D.
7	No NaOAc	23
8	[RuCl ₂ (<i>p</i> -cymene)] ₂ ^d or [Ru(OAc) ₂ (PPh ₃) ₂] instead of RuCl ₃ ·nH ₂ O and no electricity	N.D.

^a Reaction conditions: **1a** (0.50 mmol), **2a** (1.5 equiv.), RuCl₃·nH₂O (10 mol%), NaOAc (30 mol%), K₂CO₃ (2.0 equiv.), DMA (3.0 mL), 24 h, 35 °C, CCE at 2.0 mA, Zn anode, Ni cathode, undivided cell. ^b Determined by ¹H-NMR analysis using dibromomethane as the internal standard. ^c Isolated yield. ^d Catalyst loading: 5.0 mol%. CCE: constant current electrolysis, DMA: *N,N*-dimethylacetamide, N.D.: not detected.

Therefore, the direct employment of RuCl₃·nH₂O as the catalyst offers a more sustainable and user-friendly strategy for executing C–H activation. In 2007, our group first disclosed the use of arene ligand-free RuCl₃·nH₂O for *ortho*-C–H arylation.²⁴ Subsequent studies also demonstrated that RuCl₃·nH₂O can be

utilized for *ortho*-^{54–62} as well as *meta*-C–H functionalizations.^{63–65} Nevertheless, rather harsh conditions with reaction temperatures from 100–140 °C are generally required, representing a considerable limitation.

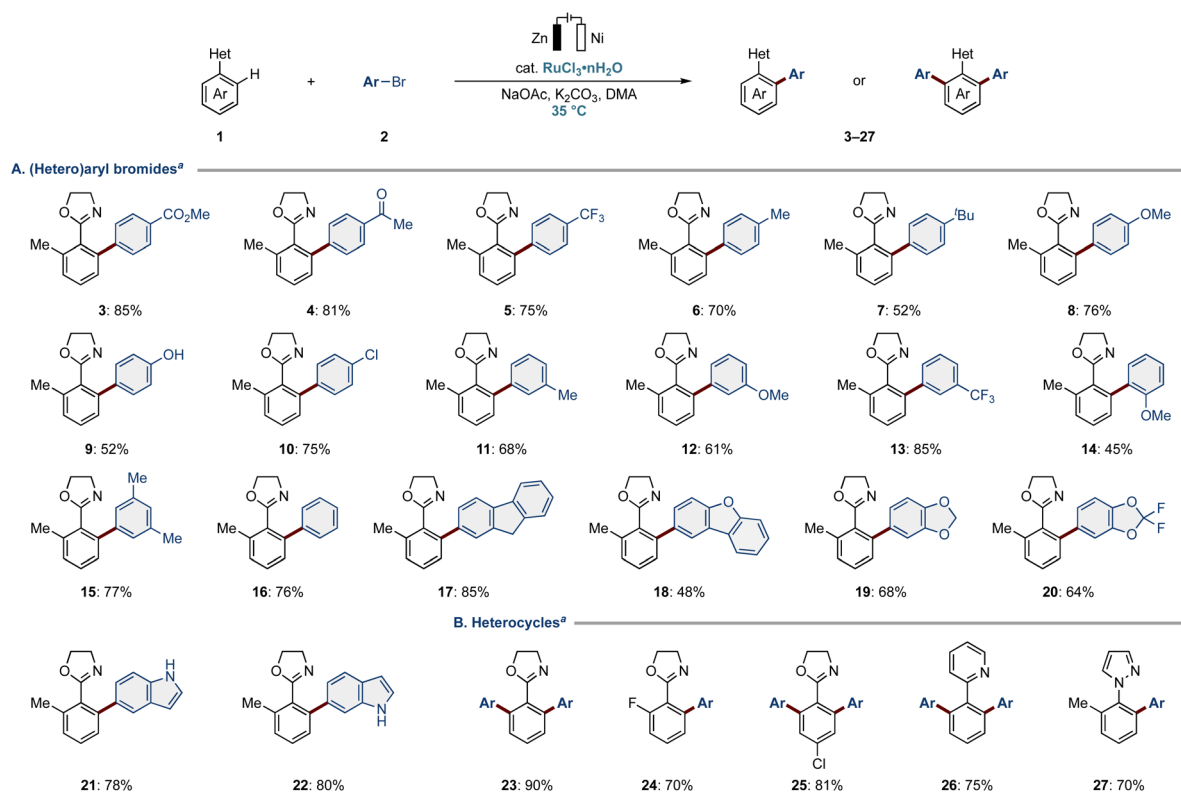


Fig. 1 (Hetero)aryl bromide and heterocycle scope. ^aReaction conditions: **1** (0.50 mmol), **2** (1.5–3.0 equiv.), RuCl₃·nH₂O (10 mol%), NaOAc (30 mol%), K₂CO₃ (2.0 equiv.), DMA (3.0 mL), 24 h, 35 °C, CCE at 2.0 mA, Zn anode, Ni cathode, undivided cell. Ar: 4-(CO₂Me)C₆H₄ for products 23–27.



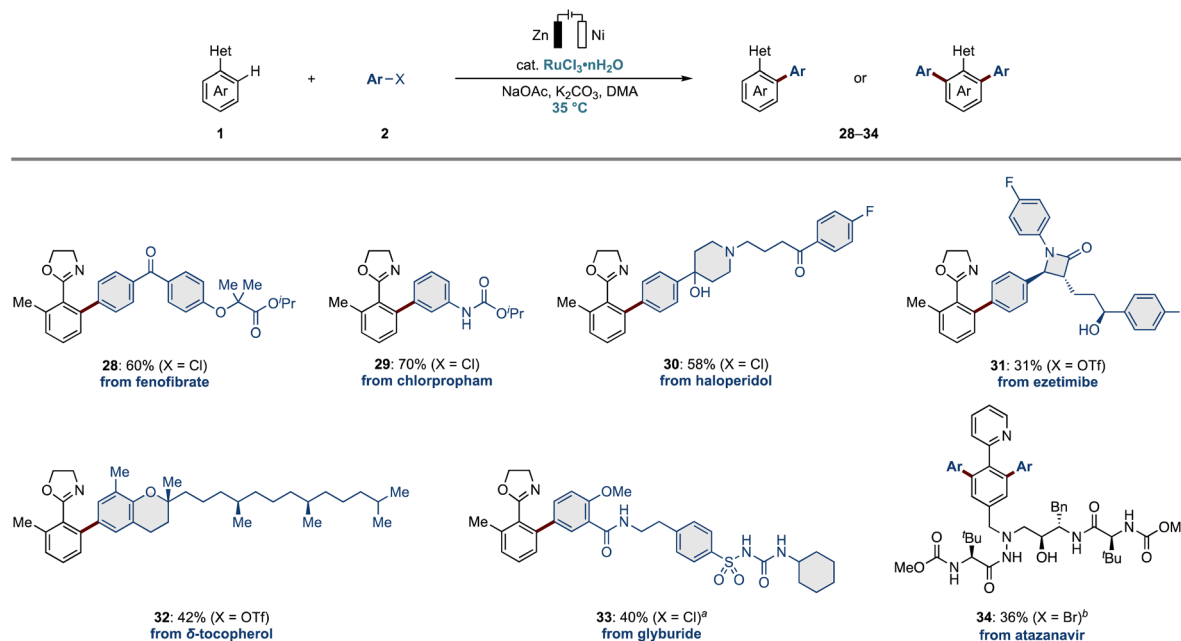


Fig. 2 Electro-late-stage diversification. General reaction conditions: **1** (0.50 mmol), **2** (1.5–3.0 equiv.), $\text{RuCl}_3 \cdot n\text{H}_2\text{O}$ (10 mol%), NaOAc (30 mol%), K_2CO_3 (2.0 equiv.), DMA (3.0 mL), 24 h, 35 °C, CCE at 2.0 mA, Zn anode, Ni cathode, undivided cell. ^a Reaction temperature: 50 °C. ^b $\text{RuCl}_3 \cdot n\text{H}_2\text{O}$: 20 mol%, NaOAc: 60 mol%, K_2CO_3 : 3.0 equiv., 70 °C. Ar: *m*-xylyl for product **34**. Bn: benzyl.

To directly unlock the inherent reactivity of ruthenium catalysis using $\text{RuCl}_3 \cdot n\text{H}_2\text{O}$, we hypothesized whether, upon the electroreduction of a ruthenium(III) species, an active ruthenium(II) intermediate could be formed,^{54,57,59} setting the stage for economically-attractive, yet user-friendly C–H activation. As a result of our studies, we, herein, disclose the direct use of $\text{RuCl}_3 \cdot n\text{H}_2\text{O}$ for C–H activations at mild reaction temperatures, enabling *ortho*-C–H arylations and *meta*-C–H alkylations across a wide array of substrates, including challenging pharmaceutical, agrochemical, and naturally-occurring molecules (Scheme 1B). Thus, we harness electricity as a sustainable reductant, eliminating the need for potentially hazardous chemical redox agents.^{66–69} A notable feature of our findings is that both a sacrificial anode or a simple amine could be employed as the terminal oxidant. Detailed spectroelectrochemical studies uncovered the key reduction of the ruthenium(III) precatalyst.

Results and discussion

Reaction optimization

To probe our original hypothesis, we performed the C–H arylation under electroreductive conditions using transformable oxazoline **1a** and aryl bromide **2a** as the model substrates in the presence of $\text{RuCl}_3 \cdot n\text{H}_2\text{O}$ as the bench-stable and commercially available precatalyst (Table 1). We thus employed NaOAc for a base-assisted internal electrophilic substitution (BIES) C–H activation manifold^{7,10} with K_2CO_3 as the stoichiometric base. We probed dipolar DMA as the solvent to ensure conductivity, along with a zinc plate as the sacrificial anode. Gratifyingly, we indeed obtained the desired arylation product **3** in 85% yield after electrolysis using a non-precious zinc plate anode and a nickel

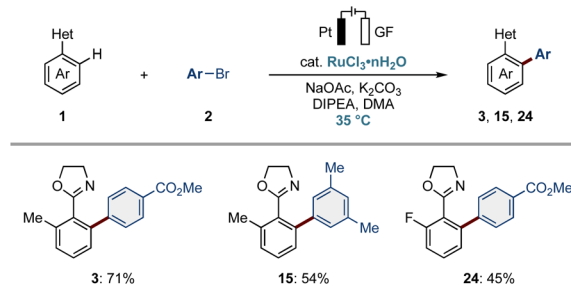


Fig. 3 Sacrificial anode-free electrochemical ruthenium-catalyzed *ortho*-C–H arylation. Reaction conditions: **1** (1.2 equiv.), **2** (0.50 mmol), $\text{RuCl}_3 \cdot n\text{H}_2\text{O}$ (10 mol%), NaOAc (30 mol%), K_2CO_3 (2.0 equiv.), DIPEA (2.0 equiv.), DMA (3.0 mL), 24 h, 35 °C, CCE at 2.0 mA, platinum anode, GF cathode, undivided cell.

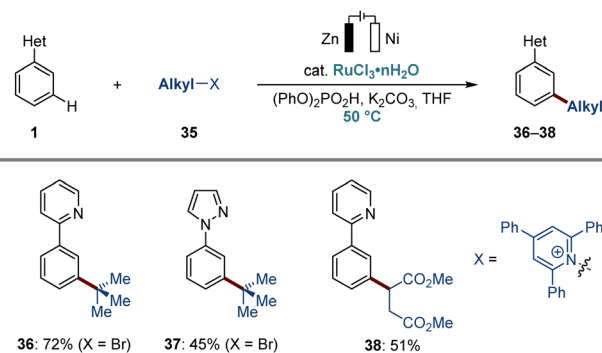


Fig. 4 Electrochemical ruthenium-catalyzed *meta*-C–H alkylation. Reaction conditions: **1** (0.50 mmol), **35** (2.0–3.0 equiv.), $\text{RuCl}_3 \cdot n\text{H}_2\text{O}$ (10 mol%), $(\text{PhO})_2\text{PO}_2\text{H}$ (30 mol%), K_2CO_3 (2.0 equiv.), ${}^t\text{Bu}_4\text{NPF}_6$ (50 mM), THF (3.0 mL), 50 °C, CCE at 1.0 mA, 4 h, and 13 h at 50 °C, Zn anode, Ni cathode, undivided cell. THF: tetrahydrofuran.



foam cathode ($j = 2.5 \text{ mA cm}^{-2}$, 1.8 F mol^{-1} , entries 1 and 2). We were delighted to observe that the reaction proceeded at $35 \text{ }^\circ\text{C}$, significantly lower than the temperatures required in previous studies using $\text{RuCl}_3 \cdot n\text{H}_2\text{O}$.^{24,54–62} *N*-Methyl-2-pyrrolidone (NMP) as the reaction medium led to a lower yield (entry 3). Other leaving groups of aryl halides, such as chloro and iodo groups, proved viable, with the bromo group being superior in the ruthenium electrocatalysis (entry 4). Thus far, chloroarenes gave inferior results, likely due to their higher bond dissociation energies (BDE).^{24,62} A control experiment without electricity highlighted the indispensable role of the electroreduction (entry 5). Likewise, no product formation or a diminished yield was observed in the absence of either $\text{RuCl}_3 \cdot n\text{H}_2\text{O}$ or NaOAc (entries 6 and 7). Particularly, the crucial presence of NaOAc suggests that carboxylate-assisted C–H activation is the operative working mode.²³ We also tested other bench-stable ruthenium(II) complexes, such as $[\text{RuCl}_2(p\text{-cymene})]_2$ or $[\text{Ru}(\text{OAc})_2(\text{PPh}_3)_2]$, albeit with limited success (entry 8).

Electrocatalysis robustness

With the optimal conditions in hand, we next explored the viable (hetero)aryl bromide scope for the electro-enabled C–H arylation (Fig. 1A). Various *para*-substituted aryl bromides were well tolerated, regardless of the electronic nature of their substituents (3–10). We were particularly pleased to find that

valuable electrophilic functional groups, such as ester (3), ketone (4), hydroxy (9), and chloro (10) groups, were fully tolerated by the electrocatalysis, without any significant signs of cross-electrophile couplings (CEC)^{70–80} induced by the electricity. Furthermore, *meta*- and more challenging *ortho*-substituted aryl bromides gave the desired arylation products likewise (11–17). To our delight, the ruthena-electrocatalysis proved compatible with hetaryl bromides, such as dibenzofuran, 1,3-benzodioxoles, and NH-free indoles (18–22).

Next, we turned our attention to evaluating heterocycle-attached arenes (Fig. 1B). The benzene-substituted oxazoline yielded the difunctionalization product **23** in excellent yield. The electrocatalysis proved tolerant of the fluoro-attached aryl oxazoline (**24**). Notably, the chloro group on the *para*-position of the aromatic ring remained intact (**25**), demonstrating the high electrocatalysis chemo-selectivity and its potential for further diversification. We were pleased to selectively obtain arylation products using pyridine and pyrazole-derived substrates (**26** and **27**).

We have confirmed, thus far, that our electrochemical C–H arylation efficiently proceeded under mild conditions to furnish various arylation products. Hence, we next explored the challenging late-stage diversification of complex molecules (Fig. 2). Thus, we employed commercially available pharmaceutical and agrochemical compounds bearing chloro leaving groups. For instance, fenofibrate and chlorpropham were successfully

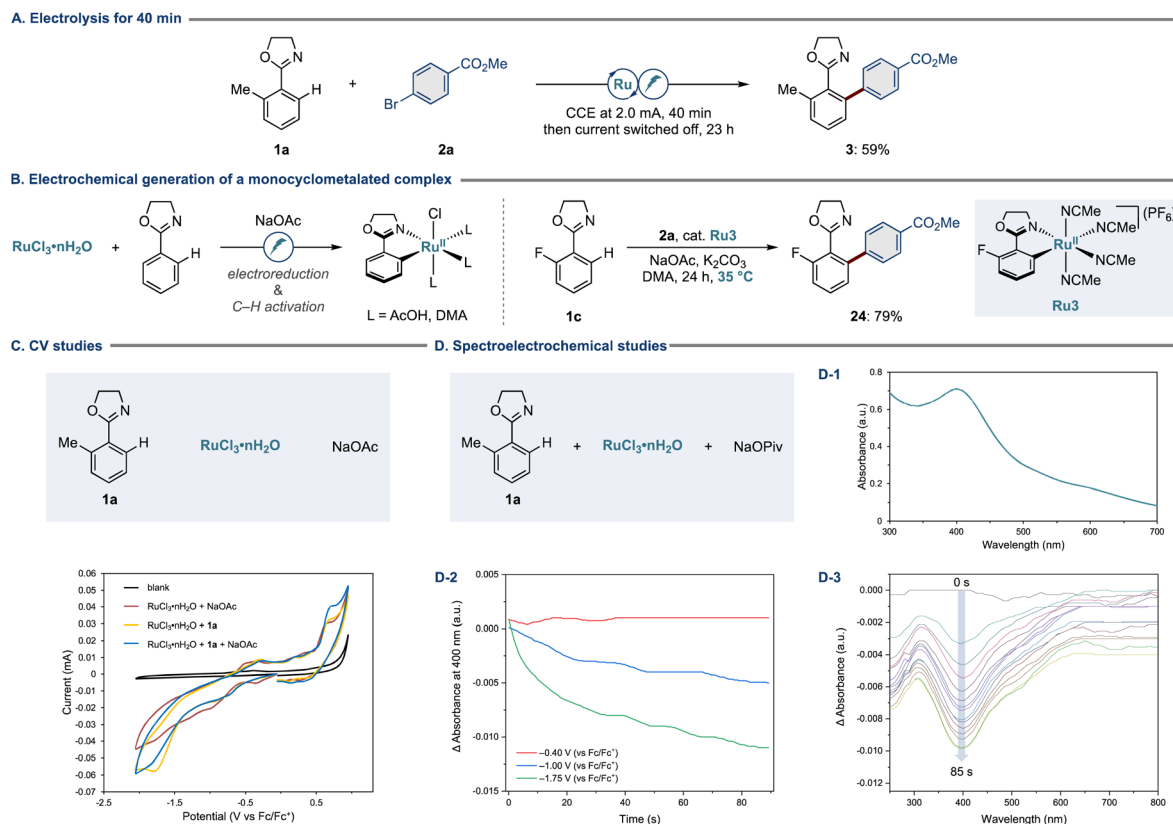


Fig. 5 (A) Electrolysis for 40 min. (B) Electrochemical generation of a monocyclusmetalated complex. (C) CV studies. (D-1) UV/vis absorption spectrum of the DMA solution containing substrate **1a** (0.13 mM), $\text{RuCl}_3 \cdot n\text{H}_2\text{O}$ (0.13 mM), and NaOPiv (0.13 mM). (D-2) Spectroelectrochemical analysis of the DMA solution containing substrate **1a** (0.2 mM), $\text{RuCl}_3 \cdot n\text{H}_2\text{O}$ (0.2 mM), NaOPiv (0.2 mM), and $t\text{Bu}_4\text{NPF}_6$ (0.1 M) at $35 \text{ }^\circ\text{C}$ under N_2 . Measurements were performed at -0.40 , -1.00 , or -1.75 V . (D-3) Spectroelectrochemical analysis performed at -1.75 V (vs. Fc/Fc^+) over 85 s.



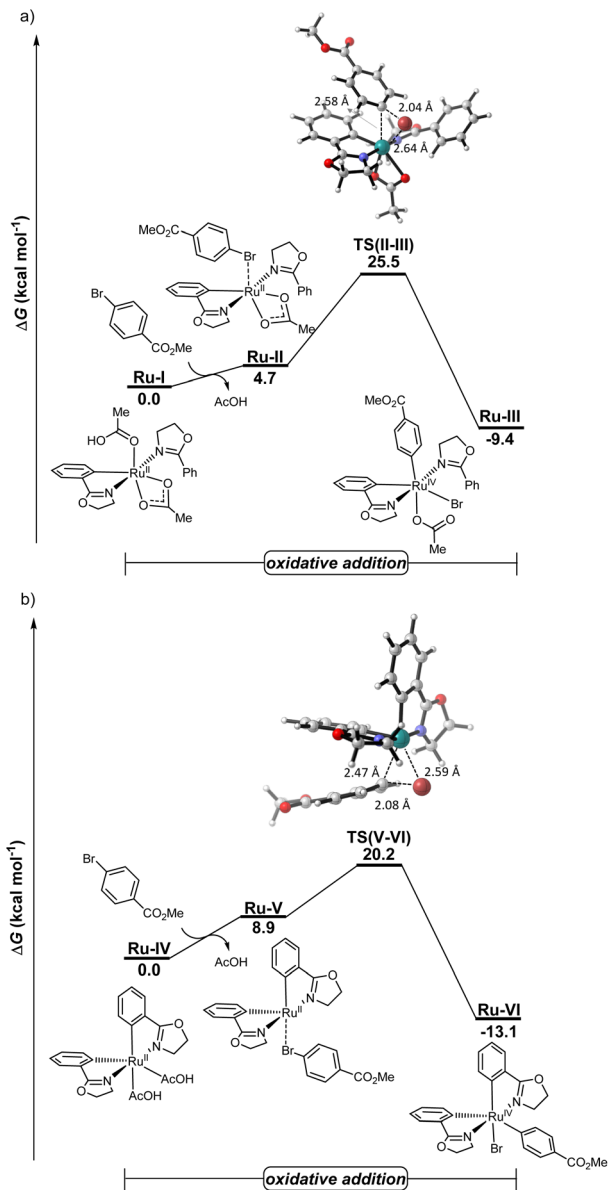


Fig. 6 Computed relative Gibbs free energies on the oxidative addition step for both (a) monocyclusoruthenated and (b) biscycloruthenated species at the PBE0-D4/def2-TZVPP-SMD(DMA)//TPSS-D3(BJ)/def2-SVP level of theory.

incorporated into the aryl oxazoline scaffolds, even when sensitive ester and carbamate functional groups were present (**28** and **29**). The drug haloperidol with a free OH-hydroxyl group was fully tolerated by the ruthenium electrocatalysis (**30**). To our delight, ezetimibe and δ -tocopherol furnished the target arylation products **31** and **32**. Furthermore, glyburide was also tolerated, leading to the arylation product bearing a sulfonyl-urea fragment, one of the important building blocks in medicinal chemistry (**33**).⁸¹ We were also pleased that the aza-peptide drug, atazanavir, underwent selective functionalization on the phenylpyridine scaffold (**34**).

To replace the zinc anode, we evaluated *N,N*-diisopropylethylamine (DIPEA) as a terminal reductant with a stable anode material.⁸² Upon experimentation,⁸³ the desired products **3**, **15**,

and **24** were selectively obtained without a sacrificial anode (Fig. 3). Detailed mass-spectrometry analysis confirmed the Hünig base (DIPEA) serving as the terminal reductant.

The ruthena-electrocatalysis was not limited to *ortho*-C-H arylations. Indeed, it also proved to be applicable to challenging *meta*-C-H alkylations, when employing secondary and tertiary alkyl (pseudo)halides (Fig. 4). By the judicious choice of additive and solvent, we accomplished the *meta*-C-H alkylations of arenes, thus giving the desired products **36** and **37**. Inspired by our previous findings,⁸⁴ we also tested the pyridinium salt derived from aspartic acid and successfully isolated the corresponding *meta*-secondary alkylation product **38**.

Mechanistic studies

Having validated the robustness of the new ruthenium electrocatalysis, we turned our attention to elucidating the *modus operandi*. First, we performed a control experiment wherein 10 mol% of electrons were supplied within the initial 40 minutes, and the current was switched off thereafter (Fig. 5A). Here, the arylation product **3** was obtained in 59% yield. This outcome suggests that electricity is primarily required to induce the formation of the key monocyclometalated ruthenium(II) intermediate (Fig. 5B, left). The involvement of such a species was verified by the experiment using a well-defined monocyclometalated complex **Ru3**, in which we obtained the desired arylation product **24** in 79% yield, further corroborating the electrochemical initiation being operative (Fig. 5B, right).

To rationalize the electrochemical features of our electrocatalysis, we conducted detailed cyclic voltammetry (CV) studies using $\text{RuCl}_3 \cdot n\text{H}_2\text{O}$, substrate **1a**, and NaOAc (Fig. 5C). Interestingly, the presence of substrate **1a** resulted in a pronounced irreversible reduction event at -1.7 V, implying coordination of arene **1a** to ruthenium. In all cases, oxidation events were observed at 0.7 V. To gain more insights, we selected specific voltage values from the cyclic voltammograms and sought to observe the potential-dependent consumption of the ruthenium(III) precatalyst by means of spectroelectrochemistry. Thus, we conducted potentiostatic analysis mode and focused on the absorption of the ruthenium(III) precatalyst at 400 nm (Fig. 5D-1). As depicted in Fig. 5D-2, whereas there was no significant change in the absorbance at 400 nm during the measurements at -0.40 and -1.00 V, spectroelectrochemical analysis at -1.75 V allowed us to detect a notable decrease in absorbance, which was also visible from the spectra with entire wavelengths (Fig. 5D-3). Overall, these observations are indicative of an electrochemical reduction of the ruthenium(III) precatalyst to afford a catalytically relevant ruthenium(II) complex. Also, electrochemical analysis by a rotating disk electrode was supportive of a ruthenium(III)/ruthenium(II) scenario.^{83,85,86}

DFT calculations

To rationalize the *modus operandi* of the electrocatalysis, detailed density functional theory (DFT) calculations were performed for the key oxidative addition step, considering both mono- and biscycloruthenated species **Ru-I** and **Ru-IV**, respectively, at the PBE0-D4/def2-TZVPP-SMD(DMA)//TPSS-D3(BJ)/



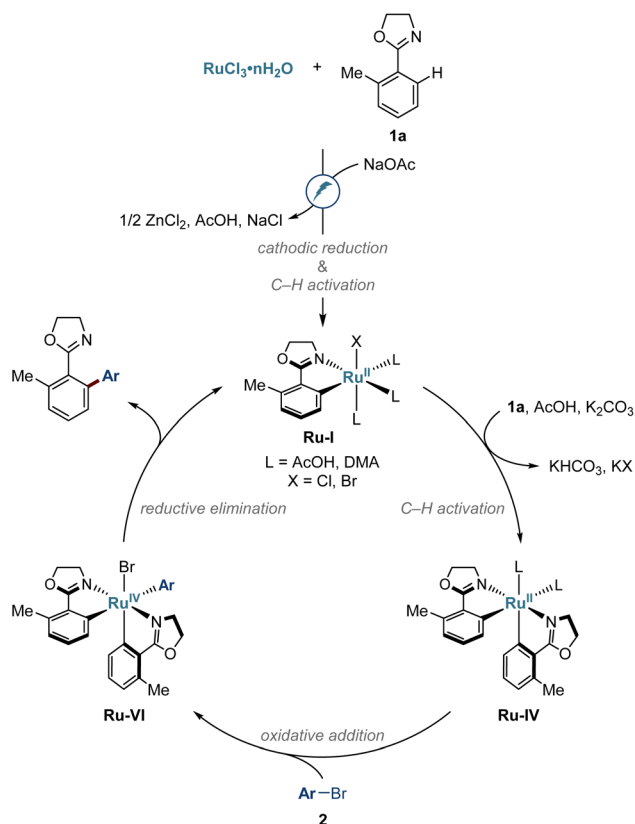


Fig. 7 Proposed mechanism.

def2-SVP level of theory (Fig. 6). The biscycloruthenated complex **Ru-IV**, generated *via* two C–H ruthenations, exhibits an energy barrier of 20.2 kcal mol^{−1} for the oxidative addition with aryl bromide **2a**, leading to the ruthenium(IV)-aryl species **Ru-VI**. Notably, the oxidative addition pathway involving the monocycloruthenated species is energetically disfavored with a considerably higher activation barrier of 25.5 kcal mol^{−1}. These results are consistent with earlier computational studies by Ackermann¹⁹ and very recent findings by Macgregor⁸⁷ for the oxidative addition occurring on the biscyclometalated ruthenium(II) intermediates.

Proposed mechanism

On the basis of our experimental and computational findings, we propose a catalytic cycle for the electro-induced C–H arylations as depicted in Fig. 7. The reaction commences upon cathodic ruthenium(III) reduction, along with carboxylate-assisted C–H activation to form complex **Ru-I**. Next, biscyclometalated intermediate **Ru-IV** is formed and undergoes oxidative addition with aryl bromide **2**. Reductive elimination from the thus formed ruthenium complex **Ru-IV** releases the arylation product and regenerates the complex **Ru-I**.

Conclusions

In conclusion, we have realized a low-temperature ruthenium-catalyzed C–H activation directly employing commercially-available RuCl₃·*n*H₂O as a resource-economical precatalyst.

The reaction provided selective access to *ortho*- or *meta*-functionalized products from a wide array of substrates, including structurally-complex drug molecules and natural products. Detailed electroanalysis provided strong support for a ruthenium(III)/ruthenium(II) manifold enabled by cathodic reduction. A sacrificial anode could be avoided. Overall, our electrocatalysis strategy offers a user-friendly and general strategy to replace the established ruthenium(II) precatalysts in the field of C–H activation chemistry to enable catalysis under exceedingly mild conditions.

Data availability

The data supporting this article have been uploaded as part of the ESI.†

Author contributions

Conceptualization, L. A.; methodology, T. M.; investigation, T. M.; spectroelectrochemical analysis, T. v. M.; rotating disk electrode experiments, T. M. and Z. L.; DFT calculations, B. Y. and J. C. A. O.; writing – original draft, all authors; writing – review & editing, all authors; funding acquisition, L. A.; resources, L. A.; supervision, L. A.

Conflicts of interest

There are no conflicts to declare.

Acknowledgements

The authors gratefully acknowledge support from the DZHK, the ERC Advanced Grant No. 101021358, the DFG (SPP2363, Gottfried Wilhelm Leibniz award to L. A.), the European Union's Horizon 2020 research and innovation program (Marie Skłodowska-Curie Grant Agreement No. 860762 to T. M.), the FCI (Kekulé-Fellowship no. 110091 to T. v. M.), and the CSC (scholarship to Z. L. and B. Y.). We thank Dr M. John (University of Göttingen) for assistance with NMR analysis and Dr H. Frauendorf (University of Göttingen) for HRMS.

Notes and references

- J. H. Docherty, T. M. Lister, G. McArthur, M. T. Findlay, P. Domingo-Legarda, J. Kenyon, S. Choudhary and I. Larrosa, Transition-Metal-Catalyzed C–H Bond Activation for the Formation of C–C Bonds in Complex Molecules, *Chem. Rev.*, 2023, **123**, 7692–7760.
- H. Liang and J. Wang, Enantioselective C–H Bond Functionalization Involving Arene Ruthenium(II) Catalysis, *Chem.–Eur. J.*, 2023, **29**, e202202461.
- K. Korvorapun, R. C. Samanta, T. Rogge and L. Ackermann, Remote C–H Functionalizations by Ruthenium Catalysis, *Synthesis*, 2021, **53**, 2911–2946.
- G. Duarah, P. P. Kaishap, T. Begum and S. Gogoi, Recent Advances in Ruthenium(II)-Catalyzed C–H Bond Activation



- and Alkyne Annulation Reactions, *Adv. Synth. Catal.*, 2019, **361**, 654–672.
- 5 J. A. Leitch and C. G. Frost, Ruthenium-catalysed σ -activation for remote *meta*-selective C–H functionalisation, *Chem. Soc. Rev.*, 2017, **46**, 7145–7153.
- 6 G.-F. Zha, H.-L. Qin and E. A. B. Kantchev, Ruthenium-catalyzed direct arylations with aryl chlorides, *RSC Adv.*, 2016, **6**, 30875–30885.
- 7 L. Ackermann, Carboxylate-Assisted Ruthenium-Catalyzed Alkyne Annulations by C–H/Het–H Bond Functionalizations, *Acc. Chem. Res.*, 2014, **47**, 281–295.
- 8 S. De Sarkar, W. Liu, S. I. Kozhushkov and L. Ackermann, Weakly Coordinating Directing Groups for Ruthenium(II)-Catalyzed C–H Activation, *Adv. Synth. Catal.*, 2014, **356**, 1461–1479.
- 9 P. B. Arockiam, C. Bruneau and P. H. Dixneuf, Ruthenium(II)-Catalyzed C–H Bond Activation and Functionalization, *Chem. Rev.*, 2012, **112**, 5879–5918.
- 10 L. Ackermann, Carboxylate-Assisted Transition-Metal-Catalyzed C–H Bond Functionalizations: Mechanism and Scope, *Chem. Rev.*, 2011, **111**, 1315–1345.
- 11 X.-Y. Gou, J. C. A. Oliveira, S. Chen, S. L. Homölle, S. Trienes, T. von Münchow, B.-S. Zhang and L. Ackermann, Ruthenaelectro-catalyzed C–H phosphorylation: *ortho* to *para* position-selectivity switch, *Chem. Sci.*, 2025, **16**, 824–833.
- 12 X. Chen, H. C. Gülen, J. Wu, Z.-J. Zhang, X. Hong and L. Ackermann, Close-Shell Reductive Elimination versus Open-Shell Radical Coupling for Site-Selective Ruthenium-Catalyzed C–H Activations by Computation and Experiments, *Angew. Chem., Int. Ed.*, 2023, **62**, e202302021.
- 13 K. Korvorapun, M. Moselage, J. Struwe, T. Rogge, A. M. Messinis and L. Ackermann, Regiodivergent C–H and Decarboxylative C–C Alkylation by Ruthenium Catalysis: *ortho* versus *meta* Position-Selectivity, *Angew. Chem., Int. Ed.*, 2020, **59**, 18795–18803.
- 14 K. Korvorapun, R. Kuniyil and L. Ackermann, Late-Stage Diversification by Selectivity Switch in *meta*-C–H Activation: Evidence for Singlet Stabilization, *ACS Catal.*, 2020, **10**, 435–440.
- 15 X.-G. Wang, Y. Li, L.-L. Zhang, B.-S. Zhang, Q. Wang, J.-W. Ma and Y.-M. Liang, Ruthenium(II)-catalyzed selective C–H difluoroalkylation of aniline derivatives with pyrimidyl auxiliaries, *Chem. Commun.*, 2018, **54**, 9541–9544.
- 16 K. Korvorapun, N. Kaplaneris, T. Rogge, S. Warratz, A. C. Stückl and L. Ackermann, Sequential *meta/ortho*-C–H Functionalizations by One-Pot Ruthenium(II/III) Catalysis, *ACS Catal.*, 2018, **8**, 886–892.
- 17 W. Liu and L. Ackermann, *Ortho*- and *Para*-Selective Ruthenium-Catalyzed C(sp²)-H Oxygenations of Phenol Derivatives, *Org. Lett.*, 2013, **15**, 3484–3486.
- 18 H. Simon, A. Zangarelli, T. Bauch and L. Ackermann, Ruthenium(II)-Catalyzed Late-Stage Incorporation of *N*-Aryl Triazoles and Tetrazoles with Sulfonium Salts via C–H Activation, *Angew. Chem., Int. Ed.*, 2024, **63**, e202402060.
- 19 T. Rogge and L. Ackermann, Arene-Free Ruthenium(II/IV)-Catalyzed Bifurcated Arylation for Oxidative C–H/C–H Functionalizations, *Angew. Chem., Int. Ed.*, 2019, **58**, 15640–15645.
- 20 M. Schinkel, I. Marek and L. Ackermann, Carboxylate-Assisted Ruthenium(II)-Catalyzed Hydroarylations of Unactivated Alkenes through C–H Cleavage, *Angew. Chem., Int. Ed.*, 2013, **52**, 3977–3980.
- 21 E. F. Flegeau, C. Bruneau, P. H. Dixneuf and A. Jutand, Autocatalysis for C–H Bond Activation by Ruthenium(II) Complexes in Catalytic Arylation of Functional Arenes, *J. Am. Chem. Soc.*, 2011, **133**, 10161–10170.
- 22 L. Ackermann, P. Novák, R. Vicente and N. Hofmann, Ruthenium-Catalyzed Regioselective Direct Alkylation of Arenes with Unactivated Alkyl Halides through C–H Bond Cleavage, *Angew. Chem., Int. Ed.*, 2009, **48**, 6045–6048.
- 23 L. Ackermann, R. Vicente and A. Althammer, Assisted Ruthenium-Catalyzed C–H Bond Activation: Carboxylic Acids as Cocatalysts for Generally Applicable Direct Arylations in Apolar Solvents, *Org. Lett.*, 2008, **10**, 2299–2302.
- 24 L. Ackermann, A. Althammer and R. Born, [RuCl₃(H₂O)_n]-Catalyzed Direct Arylations with Bromides as Electrophiles, *Synlett*, 2007, 2833–2836.
- 25 L. Ackermann, Phosphine Oxides as Preligands in Ruthenium-Catalyzed Arylations via C–H Bond Functionalization Using Aryl Chlorides, *Org. Lett.*, 2005, **7**, 3123–3125.
- 26 S. Oi, S. Fukita, N. Hirata, N. Watanuki, S. Miyano and Y. Inoue, Ruthenium Complex-Catalyzed Direct *Ortho* Arylation and Alkenylation of 2-Arylpyridines with Organic Halides, *Org. Lett.*, 2001, **3**, 2579–2581.
- 27 S. G. Ouellet, A. Roy, C. Molinaro, R. Angelaud, J.-F. Marcoux, P. D. O'Shea and I. W. Davies, Preparative Scale Synthesis of the Biaryl Core of Anacetrapib via a Ruthenium-Catalyzed Direct Arylation Reaction: Unexpected Effect of Solvent Impurity on the Arylation Reaction, *J. Org. Chem.*, 2011, **76**, 1436–1439.
- 28 S. Chen, Z. Xu, B. Yuan, X.-Y. Gou and L. Ackermann, Difunctionalization of bicyclo[1.1.0]butanes enabled by merging C–C cleavage and ruthenium-catalysed remote C–H activation, *Nat. Synth.*, 2025, **4**, 655–663.
- 29 X. Luo, P. Hou, J. Shen, Y. Kuang, F. Sun, H. Jiang, L. J. Gooßen and L. Huang, Ligand-enabled ruthenium-catalyzed *meta*-C–H alkylation of (hetero)aromatic carboxylic acids, *Nat. Commun.*, 2024, **15**, 5552.
- 30 J. Wu, N. Kaplaneris, J. Pöhlmann, T. Michiyuki, B. Yuan and L. Ackermann, Remote C–H Glycosylation by Ruthenium(II) Catalysis: Modular Assembly of *meta*-C-Aryl Glycosides, *Angew. Chem., Int. Ed.*, 2022, **61**, e202208620.
- 31 X.-Y. Gou, Y. Li, W.-Y. Shi, Y.-Y. Luan, Y.-N. Ding, Y. An, Y.-C. Huang, B.-S. Zhang, X.-Y. Liu and Y.-M. Liang, Ruthenium-Catalyzed Stereo- and Site-Selective *ortho*- and *meta*-C–H Glycosylation and Mechanistic Studies, *Angew. Chem., Int. Ed.*, 2022, **61**, e202205656.
- 32 K. Jing, Z.-Y. Li and G.-W. Wang, Direct Decarboxylative *Meta*-Selective Acylation of Arenes via an *Ortho*-Ruthenation Strategy, *ACS Catal.*, 2018, **8**, 11875–11881.
- 33 G. M. Reddy, N. S. Rao and H. Maheswaran, Highly *meta*-selective halogenation of 2-phenylpyridine with



- a ruthenium(I) catalyst, *Org. Chem. Front.*, 2018, **5**, 1118–1123.
- 34 Z. Fan, H. Lu, Z. Cheng and A. Zhang, Ligand-promoted ruthenium-catalyzed *meta* C–H chlorination of arenes using *N*-chloro-2,10-camphorsultam, *Chem. Commun.*, 2018, **54**, 6008–6011.
- 35 S. Warratz, D. J. Burns, C. Zhu, K. Korvorapun, T. Rogge, J. Scholz, C. Jooss, D. Gelman and L. Ackermann, *meta*-C–H Bromination on Purine Bases by Heterogeneous Ruthenium Catalysis, *Angew. Chem., Int. Ed.*, 2017, **56**, 1557–1560.
- 36 Z. Fan, J. Ni and A. Zhang, Meta-Selective C_{Ar}–H Nitration of Arenes through a Ru₃(CO)₁₂-Catalyzed Ortho-Metalation Strategy, *J. Am. Chem. Soc.*, 2016, **138**, 8470–8475.
- 37 J. Li, S. Warratz, D. Zell, S. De Sarkar, E. E. Ishikawa and L. Ackermann, *N*-Acyl Amino Acid Ligands for Ruthenium(II)-Catalyzed *meta*-C–H *tert*-Alkylation with Removable Auxiliaries, *J. Am. Chem. Soc.*, 2015, **137**, 13894–13901.
- 38 A. J. Paterson, S. St John-Campbell, M. F. Mahon, N. J. Press and C. G. Frost, Catalytic *meta*-selective C–H functionalization to construct quaternary carbon centres, *Chem. Commun.*, 2015, **51**, 12807–12810.
- 39 N. Hofmann and L. Ackermann, *meta*-Selective C–H Bond Alkylation with Secondary Alkyl Halides, *J. Am. Chem. Soc.*, 2013, **135**, 5877–5884.
- 40 O. Saidi, J. Marafie, A. E. W. Ledger, P. M. Liu, M. F. Mahon, G. Kociok-Köhn, M. K. Whittlesey and C. G. Frost, Ruthenium-Catalyzed *Meta* Sulfonation of 2-Phenylpyridines, *J. Am. Chem. Soc.*, 2011, **133**, 19298–19301.
- 41 L. Ackermann, N. Hofmann and R. Vicente, Carboxylate-Assisted Ruthenium-Catalyzed Direct Alkylations of Ketimines, *Org. Lett.*, 2011, **13**, 1875–1877.
- 42 A. Sagadevan, A. Charitou, F. Wang, M. Ivanova, M. Vuagnat and M. F. Greaney, *Ortho* C–H arylation of arenes at room temperature using visible light ruthenium C–H activation, *Chem. Sci.*, 2020, **11**, 4439–4443.
- 43 K. Korvorapun, J. Struwe, R. Kuniyil, A. Zangarelli, A. Casnati, M. Waeterschoot and L. Ackermann, Photo-Induced Ruthenium-Catalyzed C–H Arylations at Ambient Temperature, *Angew. Chem., Int. Ed.*, 2020, **59**, 18103–18109.
- 44 A. Sagadevan and M. F. Greaney, *meta*-Selective C–H Activation of Arenes at Room Temperature Using Visible Light: Dual-Function Ruthenium Catalysis, *Angew. Chem., Int. Ed.*, 2019, **58**, 9826–9830.
- 45 P. Gandeepan, J. Koeller, K. Korvorapun, J. Mohr and L. Ackermann, Visible-Light-Enabled Ruthenium-Catalyzed *meta*-C–H Alkylation at Room Temperature, *Angew. Chem., Int. Ed.*, 2019, **58**, 9820–9825.
- 46 G. McArthur, J. H. Docherty, M. D. Hareram, M. Simonetti, I. J. Vitorica-Yrezabal, J. J. Douglas and I. Larrosa, An air- and moisture-stable ruthenium precatalyst for diverse reactivity, *Nat. Chem.*, 2024, **16**, 1141–1150.
- 47 M. Simonetti, D. M. Cannas, X. Just-Baringo, I. J. Vitorica-Yrezabal and I. Larrosa, Cyclometallated ruthenium catalyst enables late-stage directed arylation of pharmaceuticals, *Nat. Chem.*, 2018, **10**, 724–731.
- 48 A. Dey, R. Kancherla, K. Pal, N. Kloszewski and M. Rueping, Rapid and scalable ruthenium catalyzed *meta*-C–H alkylation enabled by resonant acoustic mixing, *Commun. Chem.*, 2024, **7**, 295.
- 49 S. Trienes, S. Golling, M. H. Gieuw, M. Di Matteo and L. Ackermann, Visible light-induced ruthenium(II)-catalyzed hydroarylation of unactivated olefins, *Chem. Sci.*, 2024, **15**, 19037–19043.
- 50 P. Hauk, S. Trienes, F. Gallou, L. Ackermann and J. Wencel-Delord, Next-generation functional surfactant for mild C–H arylation under micellar conditions, *Chem Catal.*, 2024, **4**, 101146.
- 51 X. Lv, Y. Cheng, Y. Zong, Q. Wang, G. An, J. Wang and G. Li, Visible-Light-Mediated Ruthenium-Catalyzed *para*-Selective Alkylation of Unprotected Anilines, *ACS Catal.*, 2023, **13**, 7310–7321.
- 52 Y. Wang, S. Chen, X. Chen, A. Zangarelli and L. Ackermann, Photo-Induced Ruthenium-Catalyzed Double Remote C(sp²)–H/C(sp³)–H Functionalizations by Radical Relay, *Angew. Chem., Int. Ed.*, 2022, **61**, e202205562.
- 53 M. A. Bennett, T.-N. Huang, T. W. Matheson, A. K. Smith, S. Iittel and W. Nickerson, 16. (η⁶-Hexamethylbenzene) Ruthenium Complexes, *Inorg. Synth.*, 1982, **21**, 74–78.
- 54 L. Jian, H.-Y. He, J. Huang, Q.-H. Wu, M.-L. Yuan, H.-Y. Fu, X.-L. Zheng, H. Chen and R.-X. Li, Combination of RuCl₃·xH₂O with PEG – a simple and recyclable catalytic system for direct arylation of heteroarenes *via* C–H bond activation, *RSC Adv.*, 2017, **7**, 23515–23522.
- 55 Y.-L. Zou, Z.-Y. Wang, Y.-M. Feng, Y.-G. Li and E. A. B. Kantchev, Solvent and Base in One: Tetra-*n*-butylammonium Acetate as a Multi-Purpose Ionic Liquid Medium for Ru-Catalyzed Directed Mono- and Di-*o*-C–H Arylation Reactions, *Eur. J. Org. Chem.*, 2017, **2017**, 6274–6282.
- 56 B. Zhao, RuCl₃-Catalyzed Regioselective Diarylation with Aryl Tosylates *via* C–H Activation, *Synth. Commun.*, 2013, **43**, 2110–2118.
- 57 L. A. Adrio, J. Gimeno and C. Vicent, One-pot direct C–H arylation of arenes in water catalysed by RuCl₃·nH₂O–NaOAc in the presence of Zn, *Chem. Commun.*, 2013, **49**, 8320–8322.
- 58 M. Seki, Highly Efficient Catalytic System for C–H Activation: A Practical Approach to Angiotensin II Receptor Blockers, *ACS Catal.*, 2011, **1**, 607–610.
- 59 N. Luo and Z. Yu, RuCl₃·xH₂O-Catalyzed Direct Arylation of Arenes with Aryl Chlorides in the Presence of Triphenylphosphine, *Chem.–Eur. J.*, 2010, **16**, 787–791.
- 60 L. Ackermann and R. Vicente, Catalytic Direct Arylations in Polyethylene Glycol (PEG): Recyclable Palladium(0) Catalyst for C–H Bond Cleavages in the Presence of Air, *Org. Lett.*, 2009, **11**, 4922–4925.
- 61 K. Cheng, Y. Zhang, J. Zhao and C. Xie, Peroxide-Promoted Regioselective Arylation of 2-Phenylpyridines and Related Substrates with Aryl Iodides, *Synlett*, 2008, 1325–1330.
- 62 L. Ackermann, A. Althammer and R. Born, [RuCl₃(H₂O)_n]-catalyzed direct arylations, *Tetrahedron*, 2008, **64**, 6115–6124.



- 63 S. Yang, B. Yan, L. Zhong, C. Jia, D. Yao, C. Yang, K. Sun and G. Li, AIBN for Ru-catalyzed *meta*-C_{Ar}-H alkylation, *Org. Chem. Front.*, 2020, 7, 2474–2479.
- 64 C. Jia, S. Wang, X. Lv, G. Li, L. Zhong, L. Zou and X. Cui, Ruthenium-Catalyzed *meta*-C_{Ar}-H Bond Difluoroalkylation of 2-Phenoxy pyridines, *Eur. J. Org. Chem.*, 2020, 2020, 1992–1995.
- 65 G. Li, D. Li, J. Zhang, D.-Q. Shi and Y. Zhao, Ligand-Enabled Regioselectivity in the Oxidative Cross-coupling of Arenes with Toluenes and Cycloalkanes Using Ruthenium Catalysts: Tuning the Site-Selectivity from the *ortho* to *meta* Positions, *ACS Catal.*, 2017, 7, 4138–4143.
- 66 X. Cheng, A. Lei, T.-S. Mei, H.-C. Xu, K. Xu and C. Zeng, Recent Applications of Homogeneous Catalysis in Electrochemical Organic Synthesis, *CCS Chem.*, 2022, 4, 1120–1152.
- 67 M. C. Leech and K. Lam, A practical guide to electrosynthesis, *Nat. Rev. Chem.*, 2022, 6, 275–286.
- 68 C. Zhu, N. W. J. Ang, T. H. Meyer, Y. Qiu and L. Ackermann, Organic Electrochemistry: Molecular Syntheses with Potential, *ACS Cent. Sci.*, 2021, 7, 415–431.
- 69 M. C. Leech, A. D. Garcia, A. Petti, A. P. Dobbs and K. Lam, Organic electrosynthesis: from academia to industry, *React. Chem. Eng.*, 2020, 5, 977–990.
- 70 L. E. Ehehalt, O. M. Beleh, I. C. Priest, J. M. Mouat, A. K. Olszewski, B. N. Ahern, A. R. Cruz, B. K. Chi, A. J. Castro, K. Kang, J. Wang and D. J. Weix, Cross-Electrophile Coupling: Principles, Methods, and Applications in Synthesis, *Chem. Rev.*, 2024, 124, 13397–13569.
- 71 M. C. Franke and D. J. Weix, Recent Advances in Electrochemical, Ni-Catalyzed C–C Bond Formation, *Isr. J. Chem.*, 2024, 64, e202300089.
- 72 Y. Liu, P. Li, Y. Wang and Y. Qiu, Electroreductive Cross-Electrophile Coupling (eXEC) Reactions, *Angew. Chem., Int. Ed.*, 2023, 62, e202306679.
- 73 E. Richmond and J. Moran, Recent Advances in Nickel Catalysis Enabled by Stoichiometric Metallic Reducing Agents, *Synthesis*, 2018, 50, 499–513.
- 74 D. J. Weix, Methods and Mechanisms for Cross-Electrophile Coupling of Csp² Halides with Alkyl Electrophiles, *Acc. Chem. Res.*, 2015, 48, 1767–1775.
- 75 J. Gu, X. Wang, W. Xue and H. Gong, Nickel-catalyzed reductive coupling of alkyl halides with other electrophiles: concept and mechanistic considerations, *Org. Chem. Front.*, 2015, 2, 1411–1421.
- 76 D. A. Everson and D. J. Weix, Cross-Electrophile Coupling: Principles of Reactivity and Selectivity, *J. Org. Chem.*, 2014, 79, 4793–4798.
- 77 C. E. I. Knappke, S. Grupe, D. Gärtner, M. Corpet, C. Gosmini and A. J. von Wangelin, Reductive Cross-Coupling Reactions between Two Electrophiles, *Chem.–Eur. J.*, 2014, 20, 6828–6842.
- 78 S. Z. Tasker, E. A. Standley and T. F. Jamison, Recent advances in homogeneous nickel catalysis, *Nature*, 2014, 509, 299–309.
- 79 T. Moragas, A. Correa and R. Martin, Metal-Catalyzed Reductive Coupling Reactions of Organic Halides with Carbonyl-Type Compounds, *Chem.–Eur. J.*, 2014, 20, 8242–8258.
- 80 M. Durandetti and J. Périchon, Nickel-Catalyzed Electrochemical Coupling of Aryl, Heteroaryl or Vinyl Halides with Activated Alkyl Chlorides: Synthetic and Stereochemical Aspects, *Synthesis*, 2004, 3079–3083.
- 81 T. De Ventura and V. Zanirato, Recent Advances in the Synthesis of Sulfonylureas, *Eur. J. Org. Chem.*, 2021, 2021, 1201–1214.
- 82 J. Wu, R. Purushothaman, F. Kallert, S. L. Homölle and L. Ackermann, Electrochemical Glycosylation via Halogen-Atom-Transfer for C-Glycoside Assembly, *ACS Catal.*, 2024, 14, 11532–11544.
- 83 For detailed information, see the ESI.†
- 84 W. Wei, H. Yu, A. Zangarelli and L. Ackermann, Deaminative *meta*-C–H alkylation by ruthenium(II) catalysis, *Chem. Sci.*, 2021, 12, 8073–8078.
- 85 S. I. Etkind, D. A. Vander Griend and T. M. Swager, Electroactive Anion Receptor with High Affinity for Arsenate, *J. Org. Chem.*, 2020, 85, 10050–10061.
- 86 C. Amatore, M. Azzabi, P. Calas, A. Jutand, C. Lefrou and Y. Rollin, Absolute determination of electron consumption in transient or steady state electrochemical techniques, *J. Electroanal. Chem.*, 1990, 288, 45–63.
- 87 P. Domingo-Legarda, S. E. Neale, A. Carpentier, C. L. McMullin, M. Findlay, I. Larrosa and S. A. Macgregor, The Mechanism of Ruthenium-Catalyzed Directed C–H Arylation of Arenes: The Key Role of Bis-Cyclometalated Intermediates, *Angew. Chem., Int. Ed.*, 2025, 64, e202506707.

